ABSTRACT

Tiny insects use a process called ‘clap and fling’ to augment the lift forces generated during flight. The one disadvantage to using this method is the drag forces created when the wings fling apart are very large. Many tiny insects have bristled rather than solid wings, and it is thought that using the bristled wings might help reduce drag when the wings are pulled apart. The basic idea is that the wings might act as ‘leaky rakes’ during fling, meaning that the air travels through the wing reducing the drag forces generated. When the wings are in translation, they act like solid plates because the force acting normal to the wing is reduced. This mechanism is only possible if the wings flap at an intermediate Reynolds number where there is a sharp transition between arrays of cylinders acting as solids or porous media. To investigate whether or not this mechanism is feasible, we looked at leakiness for two different Reynolds numbers, ten angles of attack and three spacings. We used experiments rather than mathematical simulations study this problem due to the computational requirements of solving the Navier-Stokes equation in three dimensions for a number of configurations. From our experiments we found that leakiness decreases as the angle of attack decreases. We also found that leakiness decreases as the Reynolds number decreases. It seems likely that the wings act as solid plates for high angles of attack at higher Reynolds numbers, and as solid plates for lower angles of attack at lower Reynolds numbers.

TABLE OF CONTENTS

Introduction

Insect flight is a very active area of research in many different fields of study. This interest, in part, began as an engineering paradox. One can show using two-dimensional (2-D) steady state aerodynamic theory that a bumble bee would not be able to fly. This would be shown by comparing an insect's weight to the average amount of lift generated. In other words, if the weight of the bee is more then the lift generated by their wings, then it would be impossible for the bee to fly. This paradigm is obviously not true, and it led some physicists and mathematicians to start studying insect flight because they wanted to understand the mechanics and develop their own theory.

Biologists have also been very interested in the study of the functional morphology of insect flight. Wing design is an excellent example of convergent adaptation, and studies of the morphology are informative since the wing primarily has only one function (to generate lift). Biologists are also interested in the biological control, adaptation, and comparative morphology of insects and their flight patterns.

Engineers study the physiology, stability and maneuverability of flight. One main interest in the study of flight is for the creation of micro air vehicles and other turbomechanics. These tiny vehicles are designed mainly for military reasons. Another reason to study insect flight is to improve engineering design. There are some aspects of insect flight that humans have not been able to replicate. For example, an attribute such as hovering is a quality that man made objects have not even come close to being able to replicate.

Mathematicians view the problem of explaining how a bumble bee can fly in their own unique terms. Many observations come into play such as how various wings move individually and what kinds of forces they create in concert with another wing. These movements can be described through a mathematical language of fluid dynamics. Inherent in that language is the Reynolds number which is a dimensionless number that is used to determine different types of fluid motion. It is measured by examining a ratio of the inertial forces to the viscous forces and is defined as:

$$\mathrm{Re} = \frac{\rho l U}{\mu} \qquad (1)$$

where ρ represents the density of the fluid, l is a characteristic length (chosen as the chord length of the wing or the diameter of the bristle, depending upon the problem), U is the free stream velocity of the fluid and μ is the dynamic viscosity. Two other useful dimensionless numbers include the lift coefficient and drag coefficient. These are given by the following equations:

$$C_L = \frac{2F_L}{\rho S U^2} \qquad (2)$$

$$C_D = \frac{2F_D}{\rho S U^2} \qquad (3)$$

where F_L is the lift force acting on the wing, F_D is the drag force acting on the wing, and S is the surface area of the wing. The Reynolds number range of insect flight is about $10^1 < \mathrm{Re} < 10^3$, and for airplanes it is about $10^6 < \mathrm{Re} < 10^8$. Fluid flow acts very differently at high, medium and low Reynolds number. For this paper, what is meant by high to low Reynolds numbers (Re) is given in the following chart:

High	$Re > 10^3$	Planes
High Intermediate	$10^2 < Re < 10^3$	Large insects; bees, flies
Intermediate	$10^0 < Re < 10^2$	Tiny insects; thrips, tiny wasps
Low Intermediate	$10^{-2} < Re < 10^0$	Swimming in tiny insects, no active flying, parachuting by some seeds
Low	$Re < 10^{-2}$	Bacterial swimming

It is difficult to study the leakiness of actual insect wings because they are so small. We wish to study flight at low Re since it is different for the smallest flying insects, and it becomes less efficient as the Re decreases. Since objects with the same Reynolds number are dynamically similar, it is possible to create larger physical models of wings to study the aerodynamics. Using the similarity law, as long as the model has the same Reynolds number, it will be a sufficient representation of an actual wing.

Insect flight is very different from airplane flight because of the shape and motion of the wing and the way the vortices are formed and shed. At the beginning of each stroke, a leading edge vortex (LEV) is formed and will remain attached until the beginning of the next stroke. As demonstrated by Miller and Peskin (2004), we can better understand how lift is generated in insect flight by using a general theory of aerodynamic force in viscous flows developed by Wu (1981). Let R_∞ represent an infinite space containing a 2-D object immersed in a viscous fluid which is initially at rest. The space occupied by the fluid will be defined as, R_f and the space occupied by the object will be S. Since the total vorticity in R_∞ is initially zero, it can be shown that the total vorticity in R_∞ is zero for any finite time using the conservation of total vorticity:

$$\iint_{R_\infty} \omega(x,t)dxdy = 0 \quad (4)$$

where $\mathbf{x}$ is the position vector $\mathbf{x} = [x, y]^T$, ω is the vorticity in two-dimensional flow [ω = (dv/dx)-(du/dy)], and the fluid velocity is given as $\mathbf{u}(\mathbf{x}, t)=[u(\mathbf{x}, t), v(\mathbf{x}, t)]^T$. Note that this statement is only true when looking at vorticity over the total space occupied by both the fluid and the solid. The aerodynamic force exerted on the solid can then be approximated as:

$$F(t) = -\rho \frac{dM(t)}{dt} + \rho \frac{d}{dt} \iint_S u(x,t)dxdy \quad (5)$$

$$M_1(t) = \iint_{R_f} y\omega(x,t)dxdy$$

$$M_2(t) = \iint_{R_f} x\omega(x,t)dxdy \quad (6)$$

where $\mathbf{M} = [M_1, M_2]^T$ is the first moment of vorticity, $\mathbf{F} = [F_1, F_2]^T$ is the force acting on the wing, ρ is the density of the fluid, and S is the region occupied by the solid.

During periods of translation, the middle term in equation (5) goes to zero and what is left is as follows:

$$F_D = -\rho \frac{dM_1}{dt} = -\rho \frac{d}{dt} \iint_{R_f} y\omega dxdy \quad (7)$$

$$F_L = -\rho \frac{dM_2}{dt} = \rho \frac{d}{dt} \iint_{R_f} x\omega dxdy \quad (8)$$

where F_L is the lift force, and F_D is the drag force exerted on the solid. By using these equations we can see that the lift and drag forces are both proportional to the time rate of change of the first moment of total vorticity.

Now we consider the case of a wing which is translated from rest with an attached LEV and a trailing edge vortex that is shed. In the following equations R_f represents the region of fluid that the LEV and TEV are present in. The point of reference in these equations has the boundary stationary with the fluid moving past it in a positive direction of left to right. Along the leading edge of the wing a negative (clockwise) vorticity is formed while a positive (counterclockwise) vorticity creates the start of a vortex. The total lift force is given in the following equation:

$$F_L = \rho \frac{d}{dt} \iint_{R_f} x\omega dxdy = -\rho \frac{d}{dt} \iint_{R_P} x \mid \omega \mid dxdy - \rho \frac{d}{dt} \iint_{R_n} x \mid \omega \mid dxdy \,, \quad (9)$$

where R_n is the region of negative vorticity, R_p is the region of positive vorticity, and $|\omega|$ represents the absolute value of vorticity.

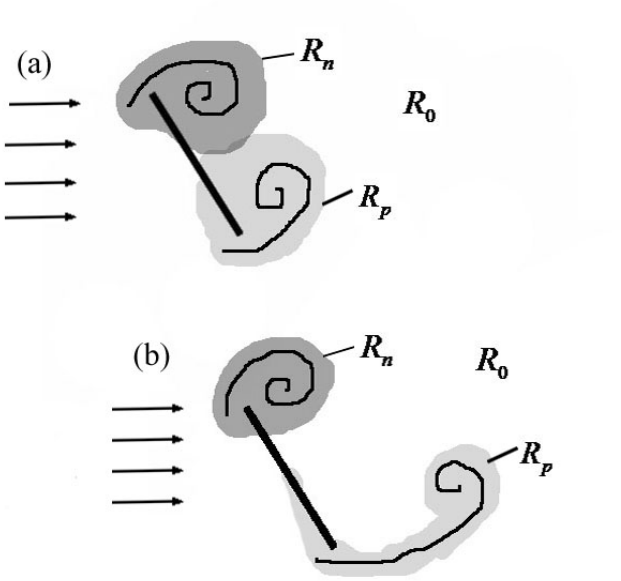

Fig. 1. Regions of positive and negative vorticity for a wing in fluid moving from left to right. R_0 represents the region of negligible vorticity, R_n represents a region of negative vorticity and R_p represents a region of positive vorticity. (a) For 4< Re < 40, leading and trailing edge vortices are formed and remain attached to the wing. (b) For Re > 40, the trailing edge vortex is shed, and the leading is vortex remains attached to the wing until stroke reversal.

Numerical simulations have shown that wake dynamics for insects flying at higher and lower Reynolds number are quite different (Peskin and Miller, 2004; Sun, 2002; Wang, 2000). The

differences in the wake dynamics also have consequences for the relative lift and drag forces generated. Wake dynamics for the lower Reynolds number case are shown in Fig 1a. Vortical near-symmetry is generated when neither the leading nor trailing edge vortices are shed until stroke reversal. Since the difference in the time rate of change of the first moment of positive and negative vorticity is minimal, lift forces are greatly reduced for insects flying at a Reynolds number below about 40. The wake dynamics for Reynolds numbers above 40 are shown in Fig. 1b. In this case, the trailing edge vortices are initially shed, and the leading edge vortices remain attached to the wing until stroke reversal. This difference in wake dynamics creates a vortical asymmetry which generates higher lift forces. It is also important to note that for Re lower than 40, drag coefficients increase significantly as the Re decreases.

The fact that the leading edge vortex (LEV) is not shed at high angles of attack was a very important step towards understanding insect flight aerodynamics. In the case of airplanes, the leading edge vortex is shed at the high angles of attack for which insects fly. This causes stall and a large drop in the lift force generated. The reason why the LEV is not shed for insects is both a function of the Reynolds number and the fact that insect wings rotate at their base in three-dimensions (3-D) (Birch et al., 2004). The fact that a relatively large LEV is formed and does not separate from the wing allows the insect to generate much larger relative lift forces than manmade aircraft flying at very high Re.

In the one wing case, lift is significantly reduced when the Reynolds number drops below about 40. However, lift is recovered when two wings perform the clap and fling motion. As mentioned above, the insects clap their wings together at the end of the upstroke, and fling their wings apart and the beginning of the downstroke (Lighthill, 1973; Weis-Fogh, 1973).

Some of the insects that use the clap and fling method are greenhouse white flies (Weis-Fogh 1975), thrips (Ellington 1999), and butterflies. The extra lift is generated when these small insects fling their wings apart at the beginning of each down stroke, creating two large leading edge vortices (see Fig 2). Miller and Peskin (2005) also found that clap and fling has a greater lift augmenting affect at lower Reynolds numbers. Perhaps this is why most tiny insects use this mechanism of lift generation.

The wings shown in Fig. 2 represent the translation and rotation that occur during clap and fling. The wings are initially clapped together, rotate along the leading edges, and then translate apart. The rotational portion of the movement creates two large leading edge vortices. The two vortices are equal in strength but have opposite signs, one positive and one negative. When the wings reach the end of their motion they are translated along a

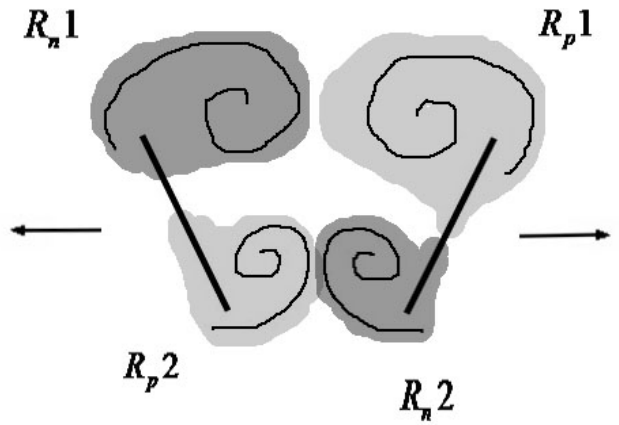

Fig. 2. Positive and negative regions of vorticity during fling. The regions denoted by R_n1 and R_n2 represent negative vorticity, while R_p1 and R_p2 represent regions of positive vorticity. The asymmetry between the LEV's and TEV's augments the lift generated.

horizontal plane creating two small trailing edge vortices. The wings in this model are being pulled apart in the direction of the arrows. The leading edge vortices are stronger then the

trailing edge vortices, which creates a vortical asymmetry leading to greater lift. The total lift acting on these wings can be described using the viscous aerodynamic theory developed by Wu (1981):

$$F_L = \rho \frac{d}{dt} \iint_{R_f} x\omega dxdy = \rho \frac{d}{dt} \iint_{R_p 1 + R_p 2} x \mid \omega \mid dxdy - \rho \frac{d}{dt} \iint_{R_n 1 + R_n 2} x \mid \omega \mid dxdy \qquad (10)$$

where |ω| represents the absolute value of vorticity. In the case described with an Eulerian perspective, the equation for total lift is written as:

$$F_L = \rho \left(\left| \frac{d}{dt} \iint_{R_n 1} x \mid \omega \mid dxdy \right| + \left| \frac{d}{dt} \iint_{R_p 1} x \mid \omega \mid dxdy \right| \right)$$

$$- \rho \left(\left| \frac{d}{dt} \iint_{R_n 2} x \mid \omega \mid dxdy \right| + \left| \frac{d}{dt} \iint_{R_p 2} x \mid \omega \mid dxdy \right| \right) \qquad (11)$$

In this equation the vortices are defined with $R_n 1$ and $R_n 2$ having vortices being pulled to the left by the wing, having a negative velocity. $R_p 1$ and $R_p 2$ are being pulled to the right by the wing, having positive velocity. In equations (9) the total lift on wing 1 and wing 2 is proportional to the magnitude of the time rate of change of the first moment of vorticity of the leading edge vorticity minus the magnitude of the time rate of change of the first moment of vorticity of the trailing edge of vorticity. It is the vortical asymmetry present as the difference in the magnitude of the leading and trailing edge vorticity generated by the clap and fling motion that produce enhanced lift during translation.

One problem with the clap and fling method is that relative drag forces increase significantly during fling for flight at a small Re. Some of possible ways to lower drag are to use flexible wings (Miller and Peskin, submitted) or to have leaky bristled wings. Interestingly, almost all tiny insects do have bristled wings. The measure of leakiness depends on the spacing of

the bristles on the wing and the Re. Sunada et al. (2002) studied a single bristled wing. They found that lift and drag changed in proportion with and without bristles. There was no apparent aerodynamic benefit of bristles for one wing flapping when compared to a solid wing. One idea suggested by Miller and Peskin (submitted) is that there may be a benefit with two wings. There may also be a benefit when different angles of attack are considered.

Miller and Peskin (submitted) proposed that the wings may act as leaky plates during the initial fling due to large forces acting normal to the wing, and as solid plates during the remainder of the stroke due to smaller forces acting normal to the wing. This would have the effect of changing the characteristic Reynolds number of the system. Cheer and Koehl (1987) described how the bristled wings in tiny insects are close to a transition point in Re where the wings go from acting as a solid at lower Re to acting as a leaky rake at higher Re (see Fig 3). Perhaps the initial fling is characterized by this higher Re range, and the translation of the wing is in this lower Re range. In order to determine whether or not this could be a drag reducing mechanism, we need a better understanding of how leakiness varies with Reynolds number, the spacing of the bristles, the length of the wing, the angle of attack, and the force acting normal to the wing.

.

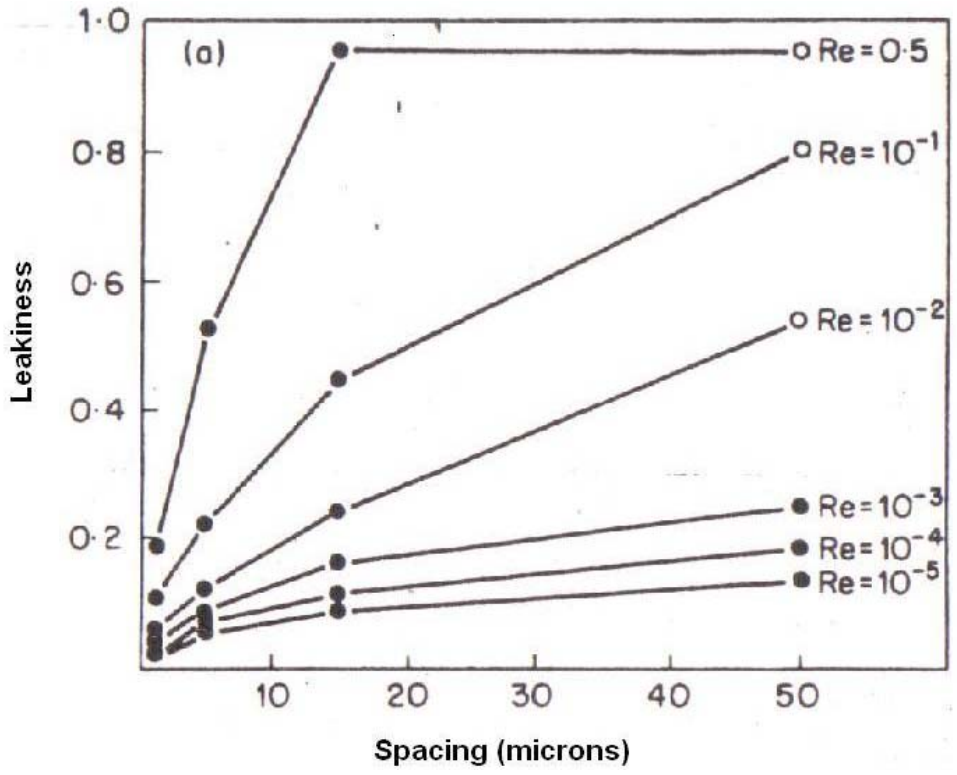

Fig. 3. A graph from the results of Cheer & Koehl (1987) showing leakiness plotted vs. the width of the spacing of the cylinders used in their experiment. The Re value is labeled at the end of each curve. Note that for tiny insect flight, the Reynolds number calculated using the diameter of a bristle may vary from about 0.01 to 0.1. There is also about a 10-20 to 1 ratio between the diameter of a bristle and the space between the bristles.

Methods

The months prior to running these experiments were spent finding a suitable design for a low to intermediate Reynolds number flow tank. Once an appropriate design was chosen, the next step was to create a physical model to simulate a bristled wing. Next, the Re was chosen to accurately reflect that of a small insect such as a thrip so that the model will be dynamically similar to an actual insect wing. The range of Re used was $10^{-3} < Re < 10^{-1}$. Note that in this case the Reynolds number for a thrips wing using the bristle width as the characteristic length is about 10^{-2}. When the characteristic length is chosen to be the chord length of the wing, the Reynolds number for thrips flight is about 10.

The flow tank was chosen to have a low Re flow, and is depicted in Fig. 4, and was attached to a Fisher Scientific, Mini-Pump Variable Flow peristaltic pump. The peristaltic pump was used to drive flow at a constant velocity through the main chamber of the pump where we placed a model wing. Because our tank operates at a low Re (Re < 1) we did not have to worry about turbulence or the formation of vortices, so flow straighteners were not necessary. Fully developed Hagen-Poseille flow developed before reaching the model. The models were made on a poster board base, and a "dish" was carved out of bottom tank to hold the model in place.

The models used to represent the wing were created out of poster board coated in epoxy glue with pins, ¼ mm in diameter, to represent the bristles on the wings. To study the leakiness of the bristles in the wings, the three different spacing of the pins which were examined were 1 cm, ½ cm and ¼ cm. Each of the different pin spacing were arranged in 9^{o} increments from 0^{o}

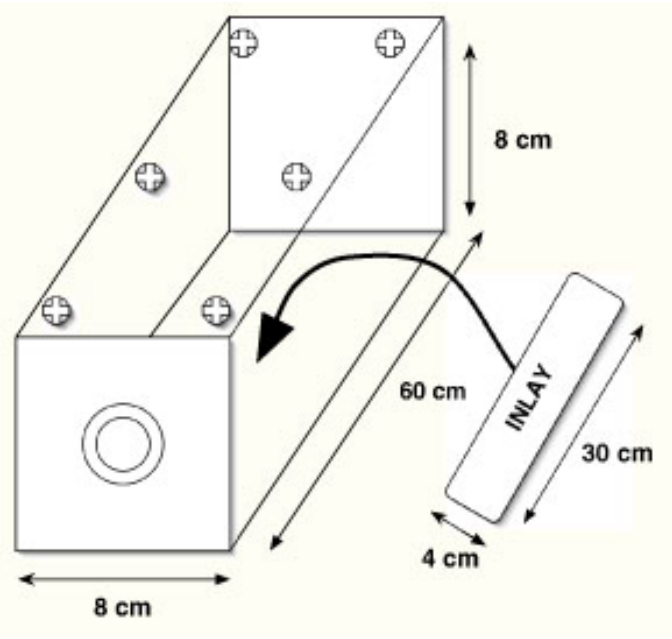

Fig. 4. Model of the flow tank used. The overall dimensions of the tank were: l x w x h = 60 x 8 x 8 cm. Dimensions for the inlay in the bottom center l x w x h = 30 x 4 x .5 cm. At each end, there are circular holes where plastic tubing was attached.

to 90^{o}, creating 11 angles for each. The middle spacing of ½ cm represents the ratio between the diameter of the thrips bristle to the space between each bristle as discussed in Cheer and Koehl (1987).

The sucrose solution which was used in the flow tank was mixed to get the appropriate range of Re. The ratio of sugar to water was 7lbs sugar to 3000ml of water. A Cannon Instrument Company viscometer No. 3B K432 was used to measure the viscosity of the sucrose solution.

For the flow visualization food coloring was added into the sucrose solution and injected into the flow with a syringe. The dye was injected parallel to the wing, the same angle of attack. As the flow moved the color through the pins, the image was captured with a Panasonic video camera (Model #: PV-GS300). The camera was placed to capture the image from a birds eye view above the flow tank and immersed wing model. It was then transferred onto a computer to analyze the data using Pinnacle Studio MediaSuite Titanium Edition on a Gateway computer.

We calculated leakiness as the ratio of the maximum velocity through the two middle pins over the maximum velocity around the wing. Also taken into account is leakiness as a function of the distance from the edge. This is different from how Cheer and Koehl calculated this value. They described leakiness as the ratio of the measured volumetric flow rate through two pins over the volumetric flow rate in the inviscid case. We also calculated

leakiness as the maximum velocity through the two pins at the end of the wing to the maximum velocity around the wing and compared it to the leakiness between the middle two pins.

Results

We took movies for the thirty-three cases described in the methods sections, each of the 11 angles at each of the three spacing were recorded. Some general trends we noticed were that leakiness decreases with decreasing angle of attack. Also, leakiness decreases towards the interior of the wing. Reduced spacing greatly reduces the flow through the wing in all cases. Also observed was that the flow to the outside of the wings bends back around towards the inside as it moves past the wing, especially in the cases where the pin spacing was the smallest.

Some representative movie clips are given in Fig. 5, A-E below. For each pair of images, the first clip is a shot taken immediately after the dye was inserted. They show the dye strip being parallel to the bristles. The next picture is one taken at a later time in the same trial. This picture was taken after the dye was carried with the flow through the pins. As you will notice in C, leakiness decreases towards the interior of the bristles. Also, the pins reduce the flow, but do not act as a complete barrier. As the angle of attack increases in D, the wing almost completely obstructs the flow as compared to the same spacing in C.

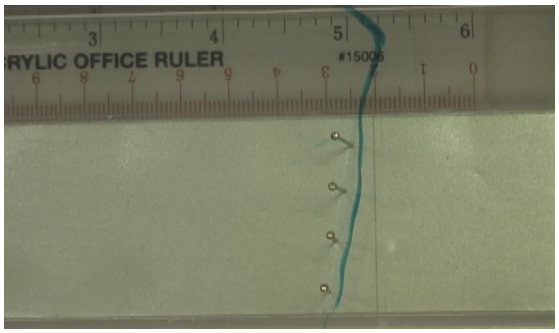
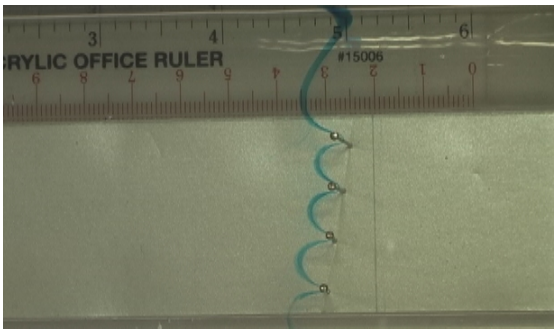

A.

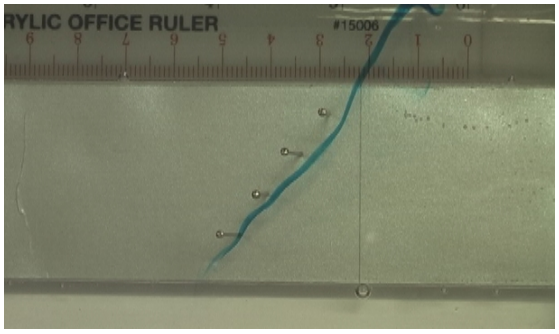
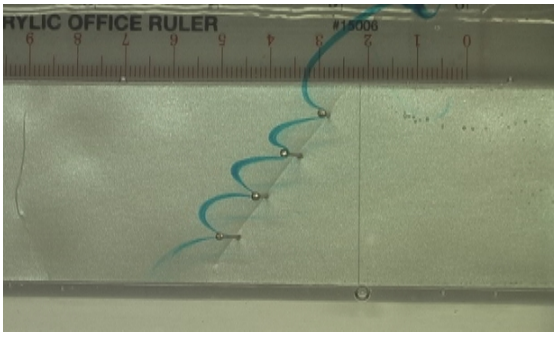

B.

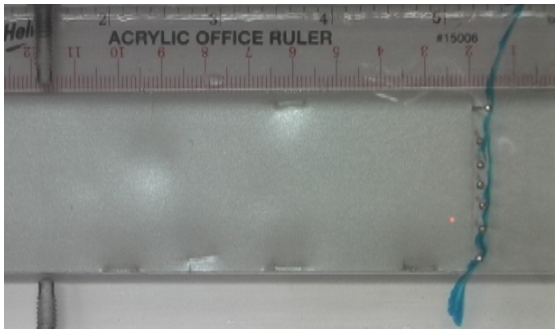
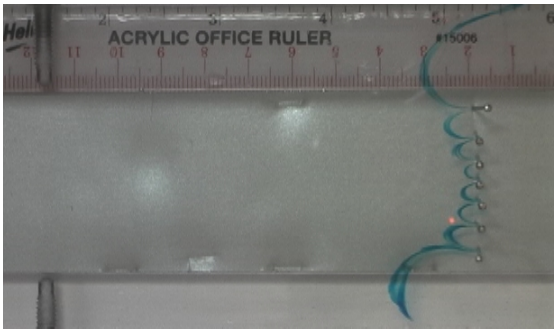

C.

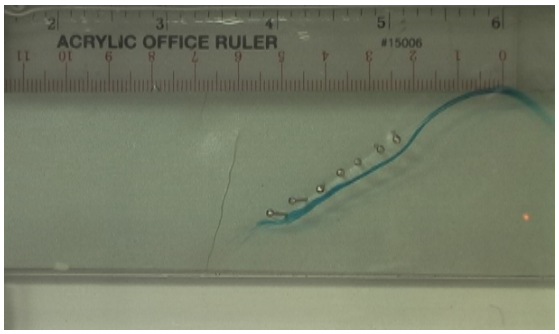
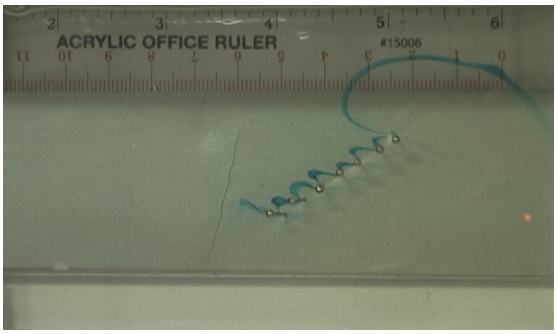

D.

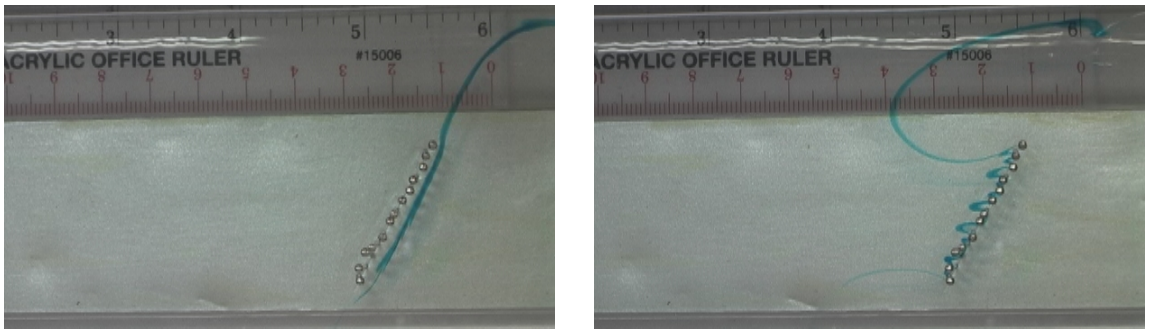

E.

Fig. 5. Images captured of fluid flow through the pins at different spacing and angles of attack. Each pair of images shows the initial insertion of die, parallel to the pins, while the second image is a demonstration of how the die was carried with the flow through the pins. The average Re for these images ranges from .023 to .047. The flow in each of the images is moving from right to left. At the top of the image is the free stream velocity which was used to compare to the flow through the pins. For images A) The pins have 1 cm spacing for 0^o, B) The pins have 1 cm spacing for 54^o, C) The pins have ½ cm spacing for 0^o, D) The pins have ½ cm spacing for 36^o, E) The pins have ¼ cm spacing for 27^o.

The leakiness as a function of angle in degrees is plotted in Fig. 6 below. Each angle was tested setting the peristaltic pump to two different speeds in order to compare leakiness at 2 Reynolds numbers. The graph in Fig. 6 shows the plots from all three spacing at the faster speed, where the average Reynolds number for all cases was about 0.047. The results we expected are verified by this graph. The 1 cm spacing allowed more flow through at a faster rate than the ½ cm and the ¼ cm spacing did. In fact, the ¼ cm spacing blocked so much flow that only the 0^o to 45^o increments were tested, because any angle higher than that would have allowed an immeasurable amount of flow. Each line on this graph represents each of the three different spacing of the pins. For all three data sets the leakiness decreases as the angle increases, as we expected to see. There is a fair amount of noise present in these graphs due to experimental error. This error could have been caused by the dye being inserted at different heights for each case. Also, it is likely that some of the pins were not

evenly spaced or standing perfectly perpendicular. There also could have been a difference with the thickness of the strip of dye inserted or the angle it was inserted at.

Fig. 6. Leakiness as a function of angle in 9 degree increments from 0^o to 90^o, for Re .047.

For the graph in Fig. 7, leakiness is expressed as a function of angle for the ½ cm spacing for Reynolds numbers of .047 and .023. By observing this graph, one can see that a greater flow rate increases the fluid flow through the pins. It can be assumed that this representation would be the same for the bristles on an actual insect wing. These data plots show how even with the different rates of flow the leakiness consistently decreased with increased angle of the pins.

The same variables of error are prevalent in this data as in Fig. 6 above, accounting for the noise in the graph. The data for 0^o and 9^o are questionable as to their accuracy. The data do not reflect what is predicted, i.e. the 0 degree plot seems too low while the 9 degree plot is too high. The margin of error in this plot was created by the specific slide chosen to measure the data. The image of 0 degrees had a very distinct pattern where the flow in the middle

pins was much less than the outer pins as demonstrated in Fig. 5C. Another factor to this error could be the amount of time that was allowed to pass in the video before capturing the image used to measure the results.

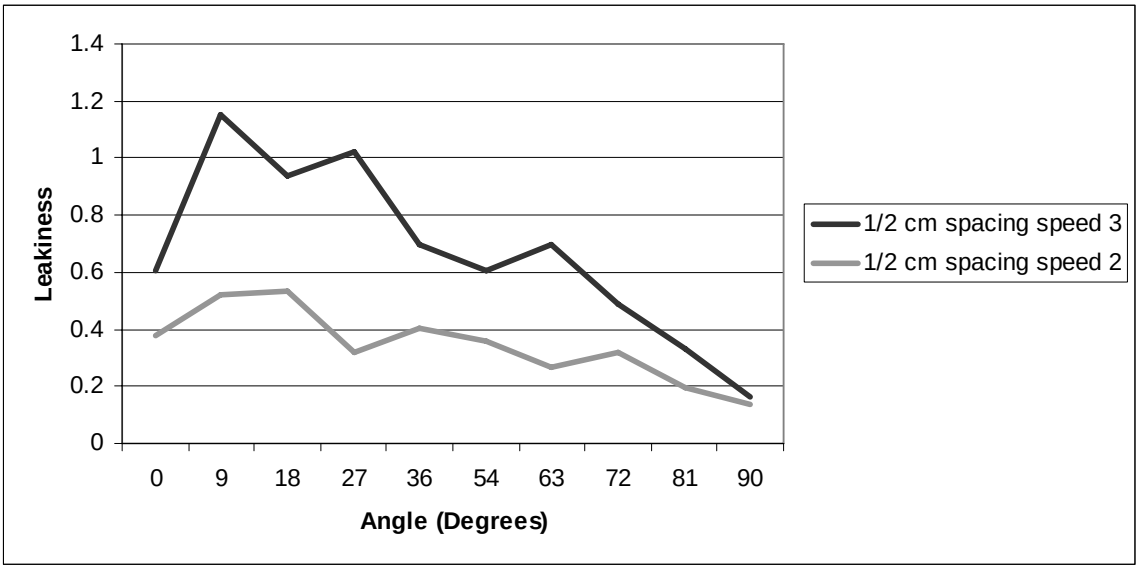

Fig. 7. Leakiness as a function of angle in 9 degree increments from 0^o to 90^o for Reynolds numbers of 0.047 (speed 3) and 0.023 (speed 2) for the ½ cm spacing.

As can be seen in Fig. 8, leakiness varies between pins. The closer to the edge, the more flow goes through the pins. In Fig. 9, leakiness as a function of angle is shown using the measurements taken from the first pin gap rather than the middle one. We found that in many cases there was more fluid allowed through the first pair of bristles than the middle ones. Each individual graph shows a significant decrease in the leakiness as the angle increased, same as our other measurements within the margin of error.

Fig. 8. 0^o degree angle with ½ cm spacing. Demonstration of the flow through the bristles being greater towards the outside of the bristles than the middle.

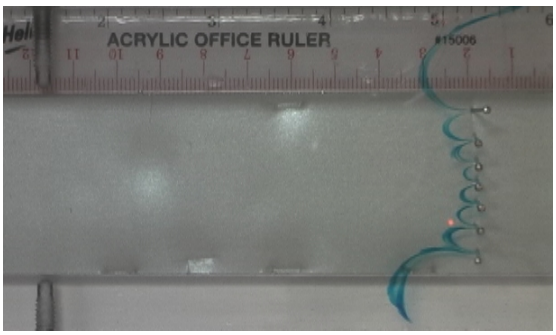

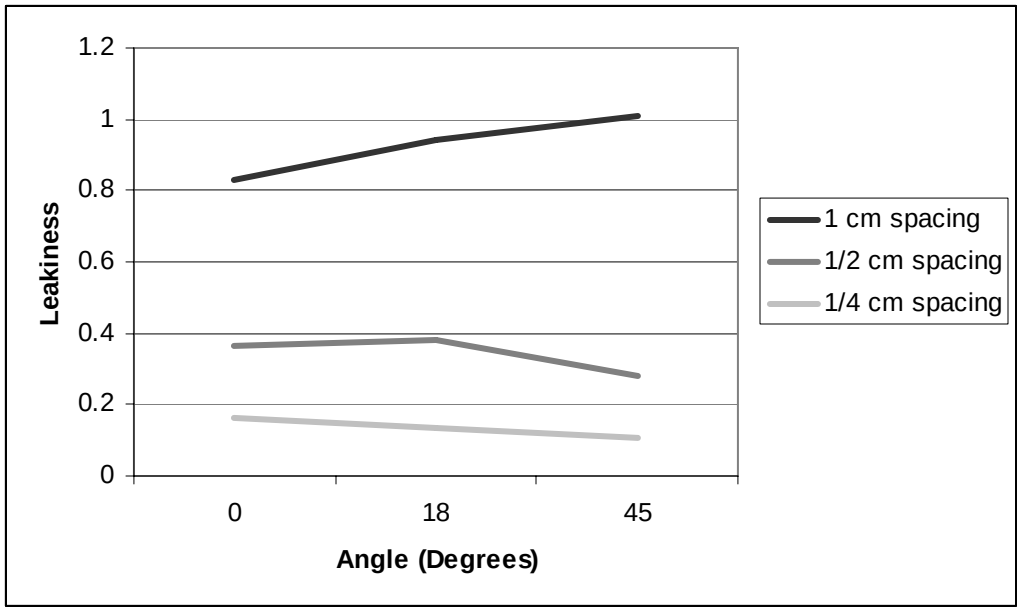

Fig. 9. Leakiness as a function of angle for the angles of 0 degrees, 18 degrees and 45 degrees, for a Reynolds number of about 0.047.

Conclusion

As mentioned before, the middle spacing of ½ cm represents the ratio between the diameter of the thrips bristle to the space between each bristle. Accordingly, the 1 cm spacing is twice as large as the spacing of the bristles in an actual thrips wing. All of the angles tested with this wing were always leaky except at really low angles of attack. With this data, having an actual wing with this ratio of spacing wouldn't work well. In the case of the ¼ cm, there

were twice as many bristles. For an actual wing perhaps this ratio isn't leaky enough at high angles of attack to be effective.

The most interesting result of this study is that leakiness changes significantly with the angle of attack. These results might be of some help in the clap and fling motion because the greatest drag forces are generated when the wings are at a 90 degree angle of attack. This is also the place where the wings will leak the most. At 45 degrees, the wings act more like a solid plate. So this effect coupled with changes in leakiness due to the force acting normal to the wing could really make the wings act like leaky rakes during fling and solid plates during the rest of the stroke.

Some of the problems that arose from using dye were that the placement of the dye in the stream was not always at the same height and the dye didn't always come out of the syringe in even amounts or perfectly parallel to the bristles. An improvement would be to upgrade to Digital Particle Image Velocimetry (DPIV). DPIV was originally developed to examine flows created for engineering purposes. They have proven useful over the last few years for the study of biological fluid studies as well. To use this technique the flow fluid must be injected with particles that will reflect light created by a laser. One advantage to using DPIV over the system that we used is that DPIV uses a high particle seeding density which produces a velocity vector field. The velocity vector field is so complete that there are no gaps in the field which will lead to a more precise study.

Of our experiments the models which best represented actual insect flight were the ones with the same Re and spacing. Another improvement would be to measure the forces generated by each model. For further research one idea that should be studied is to use a bigger range of Reynolds numbers. The Re for thrips flight is about 10^{-2}, and a good study would be to see how the results changed with a different Reynolds number. When comparing the lift across Reynolds number, one must remember to compare lift coefficients rather than straight lift.

List of Symbols and Abbreviations

F_D	drag force per unit length
F_L	lift force per unit length
l	diameter of bristle
LEV	Leading Edge Vortex
Re	Reynolds Number
U	free stream velocity of the fluid
M	first moment of vorticity
R_f	space occupied by fluid
R_n	region of negative vorticity
R_0	region of negligible vorticity
R_p	region of positive vorticity
R_∞	infinite space
S	space occupied by the object
u(x,t)	fluid velocity
x=(x,y)	position vector
μ	dynamic viscosity
ρ	density of the fluid
|ω|	absolute value of vorticity

References

Birch, J. M., Dickson, W. B. and Dickinson, M. H. (2004). Force production and flow structure of the leading edge vortex on flapping wings at high and low Reynolds numbers. *J. Exp. Biol.* **207**, 1063-1072.

Cheer, A. Y. L. and Koehl, M. A. R. (1987). Paddles and Rakes: fluid flow through bristled appendages of small organisms. *J. Theor. Biol*. **129**, 17-39.

Ellington, C. P. (1999). The novel aerodynamics of insect flight: applications to micro-air vehicles. *J. Exp. Biol*. **202**, 3439-3448.

Lighthill, M. J. (1973). On the Weis-Fogh mechanism of lift generation. *J. Fluid Mech.* **60**, 1-17.

Miller, L. A. and Peskin, C. S. (2004). When vortices stick: an aerodynamic transition in tiny insect flight. *J. Exp. Biol*. **207**, 3073-3088.

Miller, L. A. and Peskin, C. S. Flexible clap and fling in tiny insect flight, submitted to *J. Exp. Biol*.

Miller, L. A. and Peskin, C. S. A computational fluid dynamics study of 'clap and fling' in the smallest insects, submitted to *J. Exp. Biol*.

Sun, M. and Tang, J. (2002). Unsteady aerodynamics force generation by a model fruit fly wing in flapping motion. *J. Exp. Biol.* **205**, 55-70.

Sunada, S., Takashima, H., Hattori, T.,Yasuda, K. and Kiwachi, K. (2002). Fluid-dynamic characteristics of a bristled wing. *J. Exp. Biol.* **205**, 2737-2744.

Wang, Z. J. (2000). Shedding and frequency selection in flapping flight. *J. Fluid Mech.* **410**, 323-341.

Weis-Fogh, T. (1973). Quick estimates of flight fitness in hovering animals, including novel mechanisms for lift production. *J. Exp. Biol*. **59**, 169-230.

Weis-Fogh, T. (1975). Unusual mechanisms for the generation of lift in flying animals. *Sci. Am*. **233**, 80-87.

Wu, J. C. (1981). Theory for aerodynamic force and moment in viscous flows. AIAA *J*. **19**, 432-441.